

White matter connections within the central sulcus subserving the somato-cognitive action network

Georgios P. Skandalakis,^{1,†} Luca Viganò,^{2,†} Clemens Neudorfer,^{3,4,5,†} Marco Rossi,⁶ Luca Forna,² Gabriella Cerri,² Kelsey P. Kinsman,¹ Zabiullah Bajouri,¹ Armin D. Tavakkoli,⁷ Christos Koutsarnakis,⁸ Evgenia Lani,⁸ Spyridon Komaitis,⁸ George Stranjalis,⁸ Gelareh Zadeh,⁹ Jessica Barrios-Martinez,¹⁰ Fang-Cheng Yeh,¹⁰ Demitre Serletis,^{11,12,13} Michael Kogan,¹⁴ Constantinos G. Hadjipanayis,¹⁵ Jennifer Hong,¹ Nathan Simmons,¹ Evan M. Gordon,¹⁶ Nico U. F. Dosenbach,^{17,18,19} Andreas Horn,^{3,4} Lorenzo Bello,²⁰ Aristotelis Kalyvas^{8,9,‡} and Linton T. Evans^{1,‡}

^{†,‡}These authors contributed equally to this work.

See Tscherpel and Grefkes (<https://doi.org/10.1093/brain/awaf128>) for a scientific commentary on this article.

The somato-cognitive action network (SCAN) consists of three nodes interspersed within Penfield's motor effector regions. The configuration of the somato-cognitive action network nodes resembles the one of the 'plis de passage' of the central sulcus: small gyri bridging the precentral and postcentral gyri. Thus, we hypothesize that these may provide a structural substrate of the somato-cognitive action network.

Using microdissections of 16 human hemispheres, we consistently identified a chain of three distinct plis de passage with increased underlying white matter in locations analogous to the somato-cognitive action network nodes. We mapped localizations of plis de passage into standard stereotactic space to seed functional MRI connectivity across 9000 resting-state functional MRI scans, which demonstrated the connectivity of these sites with the somato-cognitive action network. Intraoperative recordings during direct electrical central sulcus stimulation further identified inter-effector regions corresponding to plis de passage locations.

This work provides a critical step towards an improved understanding of the somato-cognitive action network in both structural and functional terms. Furthermore, our work has the potential to guide the development of refined motor cortex stimulation techniques for treating brain disorders and operative resective techniques for complex surgery of the motor cortex.

1 Department of Surgery, Section of Neurosurgery, Dartmouth Hitchcock Medical Center, Lebanon, NH 03756, USA

2 Department of Medical Biotechnology and Translational Medicine, MoCA Laboratory, University of Milan, IRCCS Galeazzi Sant'Ambrogio, 20157 Milan, Italy

3 Department of Neurology Brigham & Women's Hospital, Center for Brain Circuit Therapeutics, Harvard Medical School, Boston, MA 02115, USA

4 MGH Neurosurgery & Center for Neurotechnology and Neurorecovery (CNTR) at MGH Neurology Massachusetts General Hospital, Harvard Medical School, Boston, MA 02114, USA

5 Department of Neurology, Movement Disorder and Neuromodulation Unit, Charité–Universitätsmedizin Berlin, Corporate Member of Freie Universität Berlin and Humboldt–Universität zu Berlin, Berlin 10117, Germany

Received May 17, 2024. Revised October 10, 2024. Accepted December 29, 2024. Advance access publication January 27, 2025

© The Author(s) 2025. Published by Oxford University Press on behalf of the Guarantors of Brain.

This is an Open Access article distributed under the terms of the Creative Commons Attribution-NonCommercial License (<https://creativecommons.org/licenses/by-nc/4.0/>), which permits non-commercial re-use, distribution, and reproduction in any medium, provided the original work is properly cited. For commercial re-use, please contact reprints@oup.com for reprints and translation rights for reprints. All other permissions can be obtained through our RightsLink service via the Permissions link on the article page on our site—for further information please contact journals.permissions@oup.com.

- 6 Department of Medical Biotechnology and Translational Medicine, Neurosurgical Oncology Unit, University of Milan, IRCCS Galeazzi Sant'Ambrogio, 20157 Milan, Italy
- 7 Geisel School of Medicine, Dartmouth College, Hanover, NH 03755, USA
- 8 Department of Neurosurgery, National and Kapodistrian University of Athens, School of Medicine, Athens 11527, Greece
- 9 Division of Neurosurgery, Department of Surgery, University of Toronto, Toronto, ON, Canada, M5T 1P5
- 10 Department of Neurological Surgery, University of Pittsburgh, Pittsburgh, PA 15213, USA
- 11 Cleveland Clinic Lerner College of Medicine of Case Western Reserve University, Cleveland, OH 44195, USA
- 12 Cleveland Clinic Epilepsy Center, Cleveland Clinic Foundation, Cleveland, OH 44195, USA
- 13 Department of Neurosurgery, Cleveland Clinic Foundation, Cleveland, OH 44195, USA
- 14 Department of Neurosurgery, University of New Mexico Hospital, Albuquerque, NM 87131, USA
- 15 Department of Neurosurgery, University of Pittsburgh Medical Center, Pittsburgh, PA 15213, USA
- 16 Mallinckrodt Institute of Radiology, Washington University School of Medicine, St Louis, MO 63110, USA
- 17 Department of Neurology, Washington University School of Medicine, St. Louis, MO 63110, USA
- 18 Department of Psychological and Brain Sciences, Washington University in St. Louis, St. Louis, MO 63130, USA
- 19 Department of Pediatrics, Washington University School of Medicine, St. Louis, MO 63110, USA
- 20 Department of Oncology and Haemato-Oncology, Neurosurgical Oncology Unit, University of Milan, IRCCS Galeazzi Sant'Ambrogio, 20161 Milan, Italy

Correspondence to: Aristotelis Kalyvas, MD, PhD
 Division of Neurosurgery, Department of Surgery
 University of Toronto
 4W - 399 Bathurst Street
 Toronto, ON, Canada, M5T 2S8
 E-mail: aristoteliskalyvas@gmail.com

Keywords: motor cortex; SCAN; somato-cognitive action network; plis de passage; white matter connectivity

Introduction

One of the fundamental tenets of structural-functional brain organization is that the primary motor cortex (M1) exhibits topographical organization arranged into somatotopic maps.¹ This conceptual framework has been widely popularized from Wilder Penfield's³ intraoperative direct electrical M1 stimulations which, building upon the findings by Otfrid Foerster,² elicited isolated body-effector movements following a specific spatial pattern. These findings were famously illustrated in the homunculus diagram of the motor cortex in 1948.⁴ Over time, this depiction of Penfield's homunculus fostered a misapprehension that the motor cortex comprises an uninterrupted continuum of distinct motor effector-specific regions⁵—in other words, that M1 only controls the movement of certain body parts. This understanding has been instrumental and pivotal for clinicians in localizing brain lesions associated with motor deficits.⁶ Nevertheless, this conventional wisdom poses challenges and has limitations, prompting further inquiry into the disruptive mechanism of action and related risks of surgical intervention in this region.⁷ Stroke, a leading cause of disability, often results in motor impairments due to damage in M1 or its network connections.⁶ Rehabilitation and neurostimulation techniques, such as transcranial magnetic stimulation (TMS) and transcranial direct current stimulation (tDCS), aim to enhance motor recovery by modulating M1 activity.^{8,9} Additionally, M1 is crucial for surgical interventions in patients with challenging brain tumours, where advanced intraoperative mapping and meticulous planning are essential to preserving motor function, underscoring the importance of precise structural-functional knowledge of M1.^{10,11} These insights also apply to the use of motor cortex stimulation therapies for neuropathic pain, epilepsy, obsessive-compulsive disorder (OCD), and other neuropsychiatric disorders, with only about half of such patients responding favourably to treatment.^{7,12,13}

M1 and the primary somatosensory cortex (S1) are crucially defined by their cytoarchitectonic features, which align with distinct

anatomical landmarks such as the central sulcus. Despite some inter-individual and interhemispheric variations in the superficial appearance of the central sulcus, the cytoarchitectonic boundaries that demarcate these areas show considerable consistency along the central sulcus with respect to the crests of the pre- and post-central gyri and the fundus of the sulcus.¹⁴ Additionally, M1 can be subdivided into '4 anterior' (4a) and '4 posterior' (4p) subsections, based on quantitative cytoarchitecture and receptor-binding site distributions, with each subregion offering distinct functional roles.¹⁵ This regular relationship between M1 and the gyral anatomy supports the idea that functional organization is more tightly bound to anatomical landmarks in M1 than other cortical areas.¹⁶

Originally termed by Louis Pierre Gratiolet in 1854,¹⁷ plis de passage (PDP) are cortical continuations between adjacent gyri or, in other words, sulcal interruptions. Traditionally, the central sulcus PDP have been described as 'connecting bridges' of cortex between the precentral (motor) and post-central (somatosensory) gyri.¹⁸ While Gratiolet originally described central sulcus PDP involving the motor cortex at the level of the paracentral lobule, his descriptions regarding PDP of more ventral regions of the motor cortex were vague.¹⁷ Building on this knowledge, Paul Broca subclassified PDP into three categories: the superior, middle, and inferior frontoparietal PDP.¹⁸ According to Broca, the superior and inferior PDP were more superficially situated, whereas the middle PDP ('pli de passage moyen') was located in the fundus of the central sulcus, described as transverse gyri buried within this latter structure.¹⁸ Originally, Broca defined PDP as continua between primary motor and primary sensory cortices. More recently, other authors have termed the PDP as *continua*, with further differentiation of gyral versus sulcal continua, the former being more superficial as visualized externally (with fused gyri as a variant), and the latter located more deeply.¹⁹ Although the concept of PDP encompasses not only the cortical layer but also the underlying white matter—forming an integrated structural unit—PDP-related white matter circuits have

not been thoroughly examined nor well-characterized in cadaveric or tractography studies.²⁰

The ‘somato-cognitive action network’ (SCAN), recently described by Gordon *et al.*²¹ and based on precise functional MRI findings, challenged the notion of a purely motor M1 and redefined Penfield’s homunculus. The motor homunculus does not seem like a continuous functional gradient but rather is interrupted by three functionally defined regions on each hemisphere, termed inter-effector regions.²¹ These inter-effector regions comprise the SCAN and are seemingly involved with movement and coordination of the entire body, distinct from the more traditional effector-specific regions that focus on isolated control of limbs, such as hands and feet, or even the mouth.²² SCAN may constitute part of a more general action network involving integrated body perception, pain and action planning.^{21,23} As such, SCAN sites stand in contrast to ‘effector regions’ dedicated to pure effector-specific motor control over specific limbs, which are structured as symmetric oval zones that at their centre map to fingertips, toe tips or the tip of the tongue, respectively.²¹

The SCAN operates alongside the effector-specific regions in what Gordon *et al.*²¹ refer to as an ‘integrate-isolate’ pattern, where effector-specific regions isolate fine motor control (e.g. foot, hand, mouth) while the SCAN integrates broader physiological and cognitive goals. The SCAN is characterized by three inter-effector regions per hemisphere, which exhibit strong functional connectivity both contra- and ipsilaterally, forming an interdigitated chain along the precentral gyrus. The pattern and location of the three inter-effector regions were consistently identified in all highly-sampled adults (Supplementary Fig. 1, reprinted from Gordon *et al.*²¹). It was reliably replicated within individual participants across separate datasets. Additionally, this inter-effector configuration was evident in group-averaged data from large cohorts, including 4000 participants in the UK Biobank (UKB)²⁴; 3928 participants in the Adolescent Brain Cognitive Development (ABCD) study²⁵; 812 participants in the Human Connectome Project (HCP) dataset²⁶; and 120 participants in the WU120 study²⁷ (Supplementary Fig. 2, reprinted extended data from Fig. 1C in Gordon *et al.*²¹). In contrast, the effector-specific regions demonstrate more restricted cortical connectivity to the homotopic contralateral primary motor cortex and adjacent primary sensory cortex during isolated limb movements.²¹ The SCAN demonstrates strong subcortical connectivity to regions such as the centromedian nucleus of the thalamus and the cerebellum, further supporting its role in integrating motor and cognitive functions.^{28,29} Moreover, the SCAN’s association with internal organ control, such as connectivity to the adrenal medulla, points to its involvement in coordinating autonomic and motor responses.²⁹

Both PDP and SCAN are arranged as a chain of three nodes spanning across the motor strip of the cortex. Could they have something in common? We hypothesized that PDP may provide a structural substrate of the SCAN. Here, using a comprehensive approach (Fig. 1), we analyse cadaveric human hemispheres ($n = 16$), resting-state functional MRI (fMRI) connectomes ($n \sim 9000$) and intraoperative, direct electrical stimulation recordings ($n = 33$) to investigate and compare the structural and functional organization of the human primary motor cortex.

Materials and methods

We used a multimodal approach comprising microdissections, fMRI and direct electrical stimulation (Fig. 1). We analysed 16 cadaveric human hemispheres processed through the Klingler’s method,

using a novel sharp cortical microdissection technique to investigate the location and frequency of sulcal continua that cross the central sulcus. Given the difference in structure and similarities in distribution with the SCAN nodes, we hypothesized that these white matter connections may represent a structural substrate of the SCAN network. To that end, we manually registered locations of continua onto standard stereotactic space and used the average sites as seeds in data from three large fMRI studies—the HCP,²⁶ UKB²⁴ and ABCD study²⁵—comprising a total of approximately 9000 subjects, to determine whether the sites of continua correspond to inter-effector regions in the SCAN network. Furthermore, we analysed the motor output (motor evoked potentials, MEPS) recorded intraoperatively in six exceptionally rare patients who had tumours in M1/S1. During these procedures, exposure of the anterior bank of the central sulcus was required to identify and preserve function. The analysis allowed us to reconstruct the somatotopy of the stimulated tissue, focusing on the discrimination between single-effector and multi-effector/inter-effector sites.

White matter microdissections

Sixteen normal adult cadaveric formalin-fixed hemispheres (seven right, nine left) were prepared according to Klingler’s technique,^{30–32} and subsequently studied through micro-dissection of the cortex under a surgical microscope (OPMI, Carl Zeiss) as previously described. Our dissection tools included various micro-dissectors, micro-forceps and micro-scissors, including arteriotomy and arachnoid 1.0/2.0 mm knives. Each dissection step in our study was conducted using a thickness of approximately 1 mm. Given the inherent curvature of the brain surface, dissections were performed parallel to this curvature. This method accommodates the natural anatomical contours of the brain, allowing for a more accurate morphological assessment of the structures within their native spatial relationships. In each dissection step, multiple photographs were obtained from different angles using a Nikon DSLR camera with macro lenses to illustrate the structural and topographical architecture of the PDP adequately. In all specimens, we carried out focused cortex microdissections of the pre- and post-central gyri. Here, we aimed to record the topography and morphology of the fronto-parietal PDP and investigate their spatial relationships with adjacent structures of the surface anatomy, including the sulci and gyri of the frontal lobe, the Sylvian fissure and the midline (inter-hemispheric fissure). Left-right asymmetries were examined. We progressively dissected the cortex of the pre- and post-central gyri until the depth of the sulcus was adequately exposed. After meticulous inspection for the presence of transverse gyri, the cortex of the central sulcus was dissected until a short, straight white matter connection bridging the pre- and post-central gyrus was exposed. Cortical microdissections were carried out in a stepwise manner, resembling a gradual shaving of the cortex parallel to the silhouette of the gyrus or sulcus using curved micro knives. Following exposure of the white matter connections, the surrounding cortex was dissected to illustrate the relationship between the PDP-associated white matter and the surrounding ‘U’-fibres. We recorded their number, topography, relationship with surface anatomy and distance from the midline and Sylvian fissure (SF). Finally, the patterns of the PDP were reassessed, taking our results and findings into consideration.

Functional MRI

All PDP sites were manually registered onto the cortical surface of the template defined by the ICBM 2009b NLin Asym (Montreal

Neurological Institute, MNI) space by identifying the corresponding site on an MNI surface atlas for each subject. Surface coordinates were averaged across cadavers to calculate a single average coordinate for each of the three PDP sites (top, middle, bottom). The mean Euclidean distance between corresponding PDP and SCAN nodes (as reported by Gordon *et al.*²¹) coordinates was calculated. The average surface coordinate for each of the PDP sites was used as a seed region in each of the resting-state fMRI datasets above. Furthermore, to gain insights into the cytoarchitectonic properties underlying the identified surface coordinates, we referenced their location with the Julich Brain Cytoarchitectonic Atlas.³³

For visualization purposes, network maps were thresholded to highlight the strongest functional connections. Due to differences in data acquisition and processing strategies employed, this threshold varied across the datasets. Specifically, in cortex we used UKB: $Z(r) > 1.0$; HCP: $Z(r) > 0.75$; and ABCD: $Z(r) > 0.1$. Furthermore, because the signal-to-noise ratio of fMRI is lower in subcortical structures than in cortex due to increased distance from the MR coil, more lenient thresholds were employed to visualize the strongest connections in subcortical structures than in cortex. In subcortex, we used UKB: $Z(r) > 0.75$; HCP: $Z(r) > 0.4$; and ABCD: $Z(r) > 0.03$.

Resting-state fMRI data were averaged across participants within each of three large datasets. In brief, this approach computes pairwise correlations of activity time series between every location in the brain, thus describing the whole-brain functional connectivity pattern of every brain region. These connectivity patterns are then Fisher Z-transformed to improve normality and averaged across participants within each dataset.

UK Biobank

A group-averaged, weighted eigenvectors file of an initial batch of 4100 UKB participants (aged 40–69; 53% female)—scanned using resting-state fMRI for 6 min—was downloaded from <https://www.fmrib.ox.ac.uk/ukbiobank/>. This file consisted of the top 1200 weighted spatial eigenvectors from a group-averaged principal component analysis (PCA). Details defining data acquisition and processing pipelines are available at https://biobank.ctsu.ox.ac.uk/crystal/ukb/docs/brain_mri.pdf.²⁴ This eigenvectors file was mapped to the Conte69 surface template atlas¹⁶ using the ribbon-constrained method in Connectome Workbench,³⁴ and eigenvector time courses of all surface vertices were cross-correlated.

Adolescent brain cognitive development study

Twenty minutes (4 × 5-min runs) of resting-state fMRI data, as well as high-resolution T1- and T2-weighted images, were collected from 3928 participants (9–10 years old, 51% female), who were selected as participants with at least 8 min of low-motion data from a larger scanning sample. Data collection was performed across 21 sites within the United States, harmonized across Siemens, Philips and GE 3 T MRI scanners. Acquisition parameters were previously described elsewhere²⁵ Data processing was conducted using the ABCD-BIDS pipeline (<https://github.com/DCAN-Labs/abcd-hcp-pipeline>).³⁵

Human connectome project

A vertex-wise, group-averaged, functional connectivity matrix from the HCP 1200 participants release was downloaded from db.humanconnectome.org. This matrix consisted of the average strength of functional connectivity across all 812 participants (ages 22–35; 410 female) who completed four 15-min resting-state

fMRI runs and who had their raw data reconstructed using the newer ‘recon 2’ software, with detailed acquisition and processing steps that are well-characterized in the literature.^{26,34,36,37}

Intraoperative direct electrical stimulation recordings

Six patients undergoing craniotomy at the Neurosurgical Oncology Unit of Prof. Bello (IRCCS Galeazzi—Sant’Ambrogio) for resection of a cavernoma or brain tumour requiring exposure of the anterior bank of the central sulcus were included. Patients gave formal consent to the procedures, and the study was approved by the regional ethical committee (Lombardia 1, Italy L2093). During each procedure, the craniotomy exposed the tumour area, the central sulcus, and the adjacent pre- and postcentral gyri. During cortical motor mapping, the somatotopy of M1 on the convexity was delineated by recording motor responses to direct electrical stimulation applied to the cortical surface. The sites with the highest cortical motor threshold (cMT) (i.e. negative sites, or the ones with the lowest excitability) were used as a safe entry zone. Subcortical motor mapping guided the resection by identifying corticospinal tract fibre components. Motor mapping was performed, both at the cortical and subcortical level, using high-frequency (HF) stimulation (monophasic stimulus, 500 pulse duration, inter-stimulus interval = 2–3 ms) delivered by a monopolar probe (straight tip, 1.5 mm diameter), combining the classical 5-shocks-mode (HF-To5) and the novel bistim-mode (HF-To2), as described in recent studies.^{11,38} Upon identification of a motor response, a current-intensity curve (at 5-shocks and 2-shocks) was always performed to find threshold parameters. Tumour resection in the six selected patients required exposure of a limited amount of tissue within the anterior bank of the central sulcus (M1), corresponding to the most caudal/posterior sector of the precentral gyrus buried within the sulcus. All surgeries were performed under general anaesthesia, using propofol and remifentanyl, and titrating the level of drugs to EEG and electrocorticography (ECoG) signals to avoid any burst suppression and maintain a continuous level of brain activity. See the [Supplementary material](#) for details on the monitoring protocol.

Motor evoked potentials analysis

Raw electromyography (EMG) of contralateral and ipsilateral muscles (bilateral orbicularis oris, bilateral hemitongue, mentalis, biceps brachii, flexor carpi radialis, extensor digitorum communis, abductor digiti minimi, first dorsal interosseous, bilateral abductor pollicis brevis, quadriceps, bilateral tibialis anterior, flexor hallucis brevis) was recorded with specific software (ISIS, INOMED; sampling rate, 20 kHz; notch filter, 50 Hz). For each patient, the raw data, i.e. all the MEPs recorded during the procedure, were extracted from the acquisition system, resampled at 4 kHz, and analysed offline using dedicated MATLAB software. A 100-ms window of interest from the stimulus onset was defined for each trial. The average background EMG activity and its standard deviation (± 1 SD) were then calculated from the last 25 ms of the recorded trace (i.e. from 75 to 100 ms). An MEP was considered reliable only when the EMG voltage signal exceeded the average background ± 1 SD.³⁹ The threshold parameters and the combination of muscle responses were stored for each responsive (eloquent) site.

Reconstruction of stimulation sites

The surgical procedure was recorded through the microscope view, and MRI coordinates of all the stimulated sites were acquired by

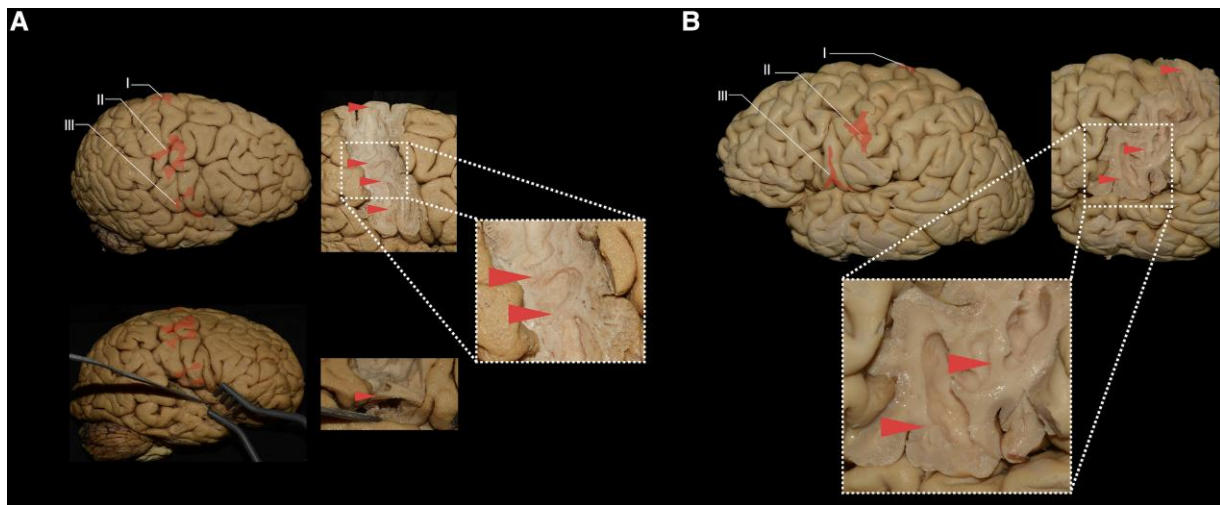


Figure 1 The plis de passage of the central sulcus. (A) Top: Lateral view of the right hemisphere of Specimen 15. The plis de passage were superimposed on the cortex in red. Right: The intra-gyral white matter connections underlying the cortical tissue of the plis de passage, as revealed through the microdissection process. Inset: Enlarged view of the middle pli de passage and a satellite middle pli de passage. Bottom: Inferior view showing the subcentral gyrus within the Sylvian fissure. A satellite inferior pli de passage was superimposed on the cortex in red. (B) Lateral view of the left hemisphere of Specimen 1 showing a striking resemblance to the somato-cognitive action network (SCAN) inter-effector pattern reported by Gordon et al.,²¹ in Fig. 7b of their study.

the neuronavigation system, allowing the visualization of the stimulation probe and the neuronavigation probe when applied on the effective sites, as well as the surrounding tissue and gyro-sulcal anatomy. A cortical surface extraction and surface volume registration were computed using the T1-weighted images loaded files into the neuronavigation system during surgery using Freesurfer software.⁴⁰ Subsequently, the results were loaded onto a Brainstorm/MATLAB toolbox,⁴¹ where the exact position of all the sites was marked as a scout on the patient's 3D MRI. With the aid of Brainstorm, each site was co-registered to the MNI space and visualized on the 3D surface reconstruction of the anterior bank of the central sulcus (ICBM 152). The MNI coordinates of each site were used to estimate the probability of overlap with the cytoarchitectonic maps available in SPM Anatomy Toolbox.^{33,42,43} The association between cytoarchitectonic maps and the type of HF-direct electrical stimulation responses (single versus inter-effector probability values) was assessed using a Mann–Whitney U-test. The region of highest probability of evoking MEPs was computed using a modified in-house version of probability kernel density estimation (PDE analysis) implemented in MATLAB.⁴⁴ Each coordinate was weighted based on the number of body-effectors involved by the stimulation to better display the voxels associated with inter-effector responses.

Population-based high definition tractography

Tracts and population-based connectivity data were obtained from a population-based tractography atlas, as described by Yeh et al.⁴⁵ The atlas provided averaged trajectories for the three subdivisions of the superior longitudinal fasciculus (SLF I, II, III) across a large cohort. For brain parcellation, we employed the HCP-Multi-Modal Parcellation (MMP) atlas, as defined in the Glasser et al. study.²⁶ This parcellation scheme subdivides the cortex into 180 regions per hemisphere, enabling precise mapping of tract coverage and cortical region interactions. All visualization and data processing were conducted using DSI Studio, an open-source diffusion MRI software as previously described.^{46,47} The software allowed for the integration of the tractography atlas with the HCP-MMP parcellation, enabling us to visualize and quantify the intersections between SLF

subdivisions and specific cortical regions. Tract-to-region intersection probability was calculated for each hemisphere to evaluate the spatial relationships between tracts and cortical regions.

Results

White matter microdissections

A chain of three distinct, short, white matter connections (superior, middle and inferior PDP) that interrupted the central sulcus at its depth was recorded in all studied hemispheres (Fig. 1 and Supplementary Table 1). The PDP predominantly comprised white matter exhibiting a morphological composition distinctly different from standard U-fibres. In contrast to the latter's delicate thinness and U shape, the white matter found within these regions exhibited a slightly deeper location, marked thickness, prominence and a less pronounced curvature when compared to the U fibres. A satellite PDP near the inferior PDP was present in 50% of the cases. Satellite PDP adjacent to both inferior and middle PDP were present in 12.5% of the cases. A superior PDP was found at the level of the SFG in 56.25% (9/16) of the cases, at the level of the superior frontal sulcus (SFS) in 31.25% (5/16) of the cases and at the level of the middle frontal gyrus in 12.5% (2/16) of the cases. The average distance from the midline was 5 ± 2.6 mm. A middle PDP was found at the level of the middle frontal gyrus in 93.75% (15/16) of the cases and at the level of the inferior frontal sulcus in 6.25% (1/16) of the cases. The mean distance from the midline to a middle PDP was 41 ± 15.1 mm, and from the Sylvian fissure 37 ± 14.1 mm. An inferior PDP was found at the level of the inferior frontal gyrus in all (16/16) of the cases. The mean distance of the inferior PDP from the Sylvian fissure was 7 ± 4.8 mm.

Functional MRI

Superimposing anatomically derived PDP to an MNI surface model corresponded to average coordinates of $x = -58.6$, $y = 1.5$ and $z = 13.8$ mm (inferior PDP); -46.1 , -9.7 , 46.5 mm (middle PDP); and -25.9 , -22.5 , 67.1 mm (superior PDP). The results are shown in Fig. 2. Individual coordinates for each cadaver are reported in

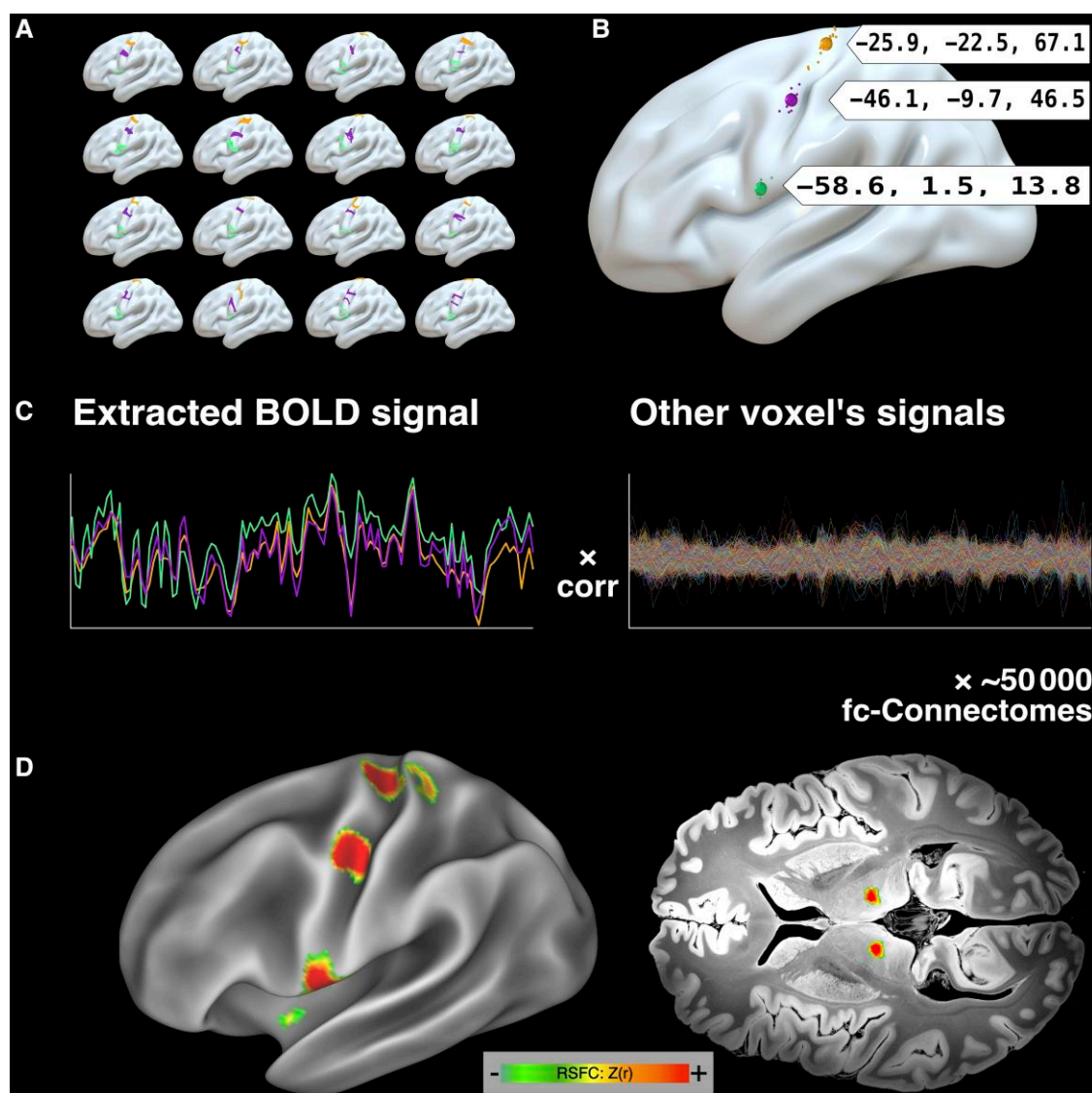


Figure 2 Mapping of plis de passage sites and functional connectivity in relation to the somato-cognitive action network. (A) The plis de passage (PDP) sites of the 16 cadaver brains were mapped and manually registered onto the brain surface template (ICBM 2009b NLin Asym), by pointing to the corresponding site on Montreal Neurological Institute surface atlas for each subject. (B) Coordinates were averaged across cadavers to calculate a single average coordinate for each of the three PDPs (top, middle, bottom), which were highly similar to the somato-cognitive action network (SCAN) inter-effector nodes reported by Gordon et al.⁹ (C) Functional connectivity (fc) of each region was computed by correlating resting-state functional MRI signals within these regions against the signals of every other brain region, and then averaging these connectivity patterns across the three regions and across all subjects within the UK Biobank (UKB), Adolescent Brain Cognitive Development (ABCD) study and Human Connectome Project (HCP) datasets. (D) Average functional connectivity map of the three PDPs across all subjects in the UKB dataset in cortex (left) and subcortex (right). The resulting map precisely matches the SCAN described by Gordon et al.⁹ See [Supplementary Fig. 3](#) for a nearly identical network maps in the HCP and ABCD datasets. BOLD = blood oxygen level-dependent; RSFC = resting state functional connectivity.

Supplementary Table 2. The mean Euclidean distance between corresponding PDP and SCAN node coordinates (as reported by Gordon et al.²¹) was 8.89 ± 2.7 mm (mean \pm SD, range: 6.2–11.5 mm). Seeding fMRI connectivity from these anatomically defined (PDP) average locations across three large datasets resulted in a network pattern in every dataset (UKB: [Fig. 2D](#); HCP and ABCD: [Supplementary Fig. 3](#)) that precisely resembled the SCAN network, including subcortical representations, such as the centromedian nucleus of the thalamus.

To gain insights into the relationship between the anatomical location of the PDP and its underlying cytoarchitecture, we derived atlas parcellations from the Julich Brain Cytoarchitectonic Atlas⁴² and superimposed the coordinates reported by our group

([Supplementary Fig. 4](#)). **Supplementary Table 3** provides an overview of the atlas allocation. Importantly, coordinates localized to border regions within primary somatosensory cortex (BA3b), primary motor cortex (BA4a) and premotor cortex (BA6), identifying the transition between areas or regions comprised of differential cell architecture.

Intraoperative direct electrical stimulation recordings

The anterior bank of the central sulcus was dissected, exposed and mapped through direct electrical stimulation in six patients ([Supplementary Table 4](#)), and the MEP response of 33 eloquent

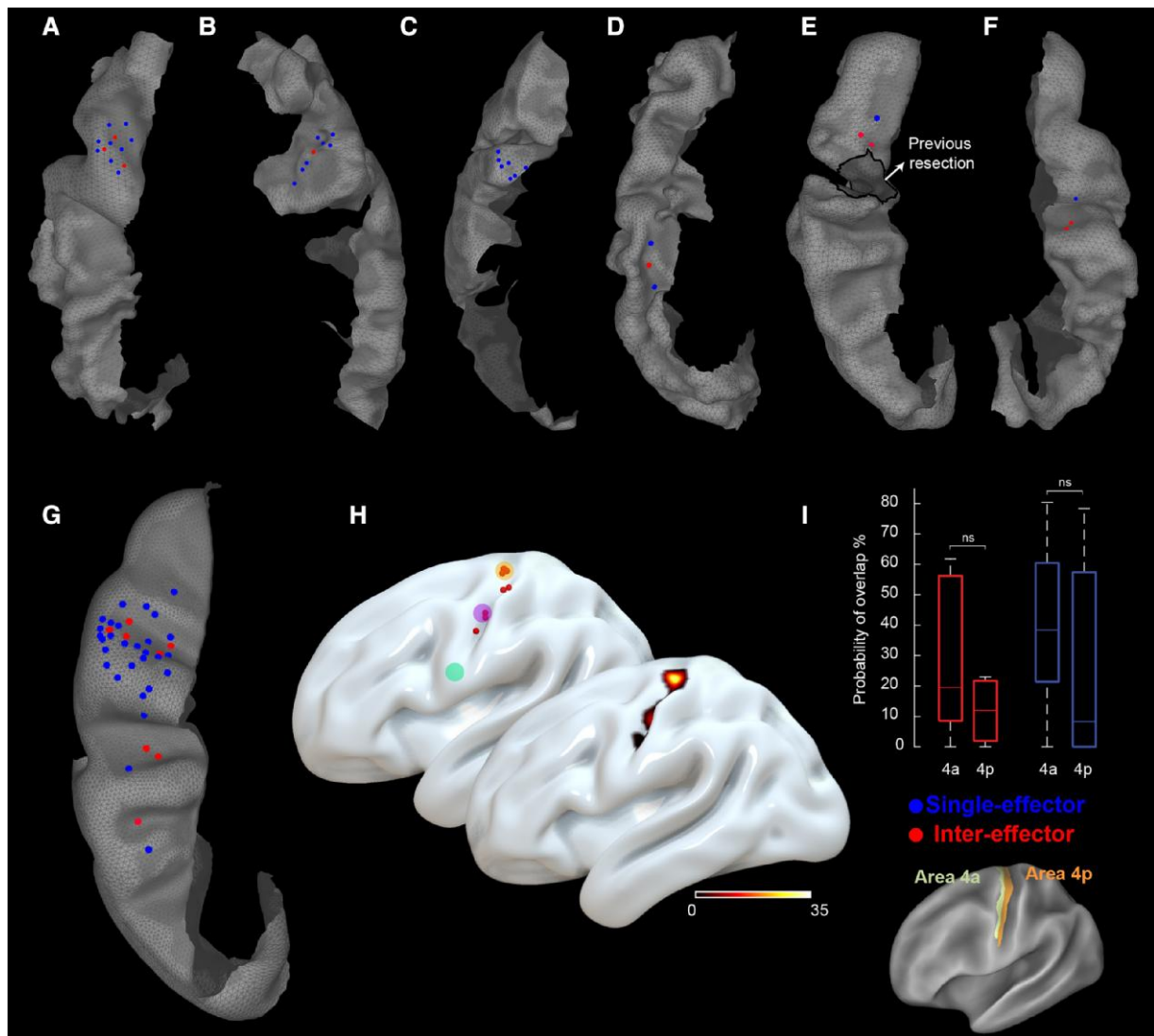


Figure 3 Intraoperative direct electrical stimulation sites. All stimulation sites for Patients 1–6 (A–F) are visualized on a 3D reconstruction of the anterior bank of their central sulcus and combined on the International Consortium for Brain Mapping (ICBM) 152 central sulcus template (G). Effector-specific sites are displayed in blue, while inter-effector sites [somato-cognitive action network (SCAN)] are displayed in red. H displays the spatial relationship between the inter-effector sites and the plis de passage (PDP) Montreal Neurological Institute (MNI) coordinates (*top*) and their probability density estimation (*bottom*). The three coloured circles in the *top* image represent the same PDP sites as in Fig. 2. (I) Box plot showing the probability of overlap between stimulation sites [inter-effector (red) versus single-effector (blue)] for the two subsectors (anterior, posterior) of area 4. Mann–Whitney U-test; not significant, ns: $P \geq 0.05$.

sites was recorded. All stimulation sites were located on the anterior bank of the central sulcus (areas 4a and 4p). Details on stimulation parameters, effectors involved, and MEPs mean amplitude are reported in [Supplementary Table 5](#). We recorded eight inter-effector sites within the region of the superior and middle PDP, in which direct electrical stimulation of single sites resulted in diffuse MEP responses involving muscle groups of different parts of the body. Given that these sites do not represent effector-specific regions, and to remain consistent with the current literature, we refer to them as inter-effector regions. Stimulation sites were overlapped with the 3D surface reconstruction of the anterior bank of the central sulcus/M1 at a single subject and population level (Fig. 3A–G). The spatial relationship between the inter-effector sites and their probability estimation with the PDP MNI coordinates is shown in Fig. 3H. Overall, we recorded eight inter-effector sites. Three of them were recorded in Patient

1. Here, direct electrical stimulation elicited reliable MEPs simultaneously in the upper limb (extensor digitorum communis muscle) and the lower limb (tibialis anterior and flexor hallucis brevis muscles) with the same threshold parameters (two stim, 8 mA). In Patient 2, HF-direct electrical stimulation revealed an inter-effector site that, when stimulated, elicited MEPs simultaneously in the proximal upper limb (biceps brachii), in distal hand muscles (flexor carpi radialis, extensor digitorum communis, abductor pollicis brevis, first dorsal interosseus, abductor digiti minimi) and the lower-limb district (tibialis anterior and flexor hallucis brevis muscles). In Patient 3, only single effector sites were found (upper-limb MEPs), possibly due to the limited amount of cortex exposed for surgical reasons, corresponding to the hand-knob sector. In Patient 4, an inter-effector site was found, evoking MEPs in distal hand muscles (flexor carpi radialis, abductor digiti minimi) and, simultaneously, in the oro-facial district (orbicularis

oris, mentalis). In Patient 5, inter-effector responses were recorded at three distinct sites. Here, MEPs were simultaneously evoked in distal hand muscles (abductor digiti minimi, first dorsal interosseus) and the lower limb (quadriceps, tibialis anterior). Finally, in Patient 6, HF-direct electrical stimulation of two different inter-effector sites elicited oro-facial and hand muscle MEPs (orbicularis oris and abductor digiti minimi). We did not record any MEPs during stimulation of the inter-effector sites with current intensity below threshold parameters (i.e. the MEPs in all responsive muscles simultaneously disappeared). Finally, in an attempt to establish a more precise anatomical location of the inter- and single-effector sites within the different sub-sectors of area 4 (4a and 4p), our analysis showed no significant differences (Fig. 3l).

Population-based high-definition tractography

In this study, we utilized population-based tractography to map the trajectories and cortical coverage of the three subdivisions of the SLF (SLF I, II, III) in relation to the precentral gyrus. We successfully reconstructed population-averaged tracts of all three subdivisions through fibre tractography and parcellated HCP-MMP cortical regions, particularly 1, 3a, 3b and 4 (Supplementary Fig. 5). SLF II and III demonstrated considerable coverage over the majority of the precentral gyrus, postcentral gyrus, and portions of the central sulci, as shown in Supplementary Fig. 5B. Specifically, SLF I showed a more restricted intersection, primarily along the lateral portions of the precentral region. Quantitative analysis of the tract-to-region connectome (Supplementary Fig. 5D) revealed high intersection probabilities for SLF II and III across the HCP-MMP regions 1, 3a and 3b, with consistently high overlap in both the left and right hemispheres (94%–100%). In contrast, SLF I exhibited minimal overlap with regions 1, 3a and 3b, and only 6%–8% overlap in the right hemisphere. In Supplementary Fig. 5E, a coronal view illustrates the distinct compartments of SLF intersection with the cortical regions. SLF II showed more medial coverage, while SLF III was predominantly lateral. This regional distinction suggests differential functional roles for SLF II and III in sensorimotor integration. Overall, these results underscore the substantial intersection of SLF II and III with precentral regions, while SLF I contributes comparatively limited (or minimal) connectivity.

Discussion

Our microdissection studies consistently revealed a chain of three distinct short white matter connections (PDP) that interrupted the depth of the central sulcus, resembling the pattern of the inter-effector regions of the SCAN, with a mean Euclidean distance between the SCAN node coordinates and PDP coordinates of 8.89 ± 2.7 mm (mean \pm SD, range: 6.2–11.5 mm). Seeding fMRI functional connectivity from group-averaged PDP locations in three large datasets ($n = 9000$) functional connectomes resulted in a pattern that precisely matched the SCAN network. Central sulcus locations at which intraoperative electrical stimulation caused movement across multiple body parts (not effector specific) overlapped with the SCAN inter-effector nodes identified by functional connectivity and the PDP identified by white matter microdissection. Our comprehensive approach utilizing microdissections, resting state MRI connectomes and intraoperative mapping studies indicated that the PDP of the central sulcus are subserving the SCAN nodes as a structural, anatomical substrate.

Distinctive structural segments of the primary motor cortex

Although traditional literature has focused on describing the superficial cortical folding associated with PDP,^{17,18} our findings herein broaden its structural description by extending the understanding of the white matter connections within PDP architecture. This expanded view can be supported by studies that identified PDP as cortical landmarks linked with regions of increased, short-range white matter connectivity, linking adjacent gyri; thus, PDP could be considered an integrated structural unit comprised of both grey and white matter.²⁰ Research has demonstrated a concentration of short fibres in primary cortices, suggesting that PDP might represent potential key elements in the intricate network of connectivity supporting complex motor and cognitive functions.⁴⁸

Our findings show that central sulcus PDP constitutes an interdigitated chain down the precentral gyrus, similar to the SCAN network sites described by Gordon et al.²¹ Analogous to the newly described SCAN network loci, PDP interrupt the central sulcus, and hence M1, at specific and remarkably similar sites. We find that PDP are located within the depths of the central sulcus, reinforcing their similarity to the SCAN regions. This assertion is supported by findings of functional connectivity of the inter-effector regions into the fundus of the central sulcus.²¹ The depth of the central sulcus has been implicated in proprioception,⁴⁹ a function potentially supported by the SCAN network.²¹ Here, we show that PDP constitute true white matter axonal connections moving beyond traditional descriptions of unique cortical folding patterns interrupting the central sulcus. Furthermore, we highlight their role as integrated cortico-subcortical functional units. On a cytoarchitectonic level, PDP mapped to border regions within the primary somatosensory cortex (BA3b), primary motor cortex (BA4a) and premotor cortex (BA6), localizing to transition zones between cytoarchitectonic labels. This finding may indicate a possible extension of the inter-effector concept to the cytoarchitectonic level, where structure, function and cytoarchitecture could play a role in facilitating integrated body perception, action planning and execution.

Our microdissection findings demonstrate that central sulcus PDP predominantly comprise substantial volumes of white matter (Fig. 1). The morphological composition of the PDP (denser, less curved, more prominent) distinctly deviates from standard U-fibres, suggesting that PDP may not connect the superficial/lateral parts of M1 and S1. PDP, as structural units, might have more extensive connectivity patterns.^{48,50,51} Nevertheless, it is crucial to note that both the SCAN regions and the PDP as delineated by our dissections, do not establish connections to lateral/superficial regions of the postcentral gyrus. It is conceivable that the connection between M1 and S1 within effector-specific regions might be mediated by U-fibres, given their characteristic superficial termination patterns. Satellite connections that we often found close to the middle and inferior PDP in some of our cases may suggest structural variations linked to case-specific SCAN node volume differences, as reported by Gordon et al.²¹ This could indicate that in individuals with larger SCAN nodes, auxiliary PDP might be present, contributing to these subject-specific volumetric differences.

The SCAN network is characterized by its wide and extensive connectivity, mapping across various cortical regions to support complex motor and cognitive functions.²¹ In contrast, PDP are more localized. Despite this apparent difference in scale, the observed similarity between the locations of PDP and SCAN nodes is compelling and suggests a potential structural basis for the SCAN's inter-effector nodes. This view is supported by research demonstrating that

functional brain connectivity often reflects broader and more extensive networks than direct structural connections alone.^{50,52} Studies by Honey *et al.*⁵⁰ have shown that functional connectivity can emerge from indirect pathways and neural synchronization across distant brain networks, leading to broader connectivity patterns than those predicted by direct structural connections alone. Similarly, Damoiseaux and Greicius⁵² emphasized that functional connectivity networks, such as those observed in resting-state fMRI, often encompass wider regions than their structural counterparts, suggesting that functional networks may be more extensive than the underlying structural connectivity. Functional networks can reflect complex, dynamic interactions that extend beyond direct anatomical connections, reinforcing the idea that functional connectivity may not always align perfectly with structural connectivity.⁵¹ Therefore, it is plausible that PDP contribute to the integrative functions of SCAN. This perspective underscores the importance of considering both cortical and white matter components when examining the structural foundations of functional networks.

Finally, in considering alternative structural networks, the presence of three inter-effector regions might superficially suggest a comparison with the three branches of the SLF. However, a more detailed anatomical analysis highlights key differences. SLF II and III are lateral to the corticospinal tract, while SLF I is medial and distant from SCAN nodes as per Gordon *et al.*^{53–55} Population-based tractography⁴⁵ further shows minimal overlap between SLF I and SCAN nodes, supporting distinct differences in their respective underlying anatomical pathways, despite some apparent superficial similarities (Supplementary Fig. 5).

Direct brain mapping: navigating past challenges and acquiring insights

Direct electrical stimulation stands as an indispensable technique in neuroscience.⁵⁶ The conceptual framework of a motor homunculus stemmed from Penfield's intraoperative, direct electrical stimulations of the precentral gyrus.⁵⁷ However, the primary motor cortex folds within the central sulcus. It thus also occupies the anterior bank of the central sulcus which according to Penfield was not exposed during his intraoperative mapping.^{58,59} Direct electrical stimulation of the anterior bank of the central sulcus requires dissection and exposure, which becomes essential when contemplating resective surgery for lesions in this region. Due to the technical complexity and inherent complication risks, lesions in this anatomical area have often been deemed inoperable. Recent advances in motor mapping strategies have challenged this view, reporting the feasibility of surgery within M1 and the corticospinal tract with a very low morbidity rate.^{11,38} Our findings show that, although exceptionally rare, within the context of appropriate indications and with the proper technique, the anterior bank of the corticospinal tract can be exposed and mapped through direct electrical stimulation. Moreover, our findings show that the primary motor cortex is indeed composed of effector-specific (foot, hand, mouth) motor regions and SCAN inter-effector regions important for whole-body action implementation.

The SCAN inter-effector sites were located at the transition between areas 4a and 4p, intermingled with effector-specific sites. The present data do not allow us to make conclusive remarks about a potentially different organization, in terms of somatotopy, between anterior and posterior area 4. However, our findings might suggest that the human motor system hosts a fundamental action-centred organization, or hierarchy, within its well-known effector-specific representation. This evidence is in line with both previous

electrophysiological studies with direct stimulation of the human precentral gyrus convexity,^{39,56} and with intracortical microstimulation of the non-human primate motor cortex, able to evoke ethologically relevant actions (e.g. 'bring to the mouth' movements)²⁸ and complex co-activation of multiple muscles, possibly supporting natural behaviours.⁶⁰ Moreover, the presence of SCAN inter-effector regions within areas 4a and 4p is consistent with recent direct mapping data obtained with intracerebral stereo EEG electrodes along the anterior bank of the central sulcus, which also challenge the notion of a purely body movement-centred, human motor cortex.²² The authors reported the existence of sites in the central sulcus, interspersed between foot-, hand- and mouth-specific regions, that were non-specifically electrophysiologically active during movement execution with any limb: the feet, hands and mouth. Here, we provide data confirming this newly described anatomo-functional organization by EMG recordings during direct electrical stimulation.

Expanding beyond a pure motor M1 model reinstates treatment opportunities

We provide evidence on the topography, morphology and functional connectivity of the PDP of the central sulcus. Our data suggests that these connections correspond to the newly described inter-effector regions within the SCAN network. Potentially, our results add an anatomical interpretation to their functional description. The presented results further add clarity to the relationships between PDP, the SCAN network and effector-specific motor regions in showing that PDP fall onto inter-effector regions of the SCAN network. The localization and number of PDP varies across subjects, and PDP mostly consists of white matter, thus representing true white matter connections. This work provides a critical step towards precisely mapping the SCAN nodes through structural imaging and could guide the development of refined motor cortex stimulation strategies and operative techniques for complex surgery of the somatomotor cortex, which is essential to preserving motor function.^{10,11} Moreover, the SCAN was suggested to be involved in the processing of pain signals.²¹ Motor cortex stimulation can treat patients with neuropathic pain, yet only 40% of patients respond to this treatment. More specific neuromodulatory targeting of the PDP might increase the therapeutic effects of M1 stimulation for the treatment of neuropathic pain or other neuropsychiatric disorders.^{7,12} Given the pivotal role of M1 in stroke rehabilitation, modulating PDP activity may also enhance motor recovery outcomes.^{8,9} Furthermore, recent findings suggest that the SCAN is critically involved in the pathophysiology of Parkinson's disease and its brain stimulation treatments, making the PDP a promising candidate target for neuromodulation.⁶¹

Limitations and future directions

Despite the significant insights provided by our study, several limitations should be acknowledged. First, the sample size of cadaveric human hemispheres ($n = 16$), while providing valuable anatomical details, may not capture the full variability present in the broader population. Second, our resting-state fMRI connectomes ($n \sim 9000$ across three datasets) and intraoperative direct electrical stimulation recordings ($n = 33$) provide robust functional data, yet the integration of these modalities into a cohesive model of SCAN functionality requires further validation. Third, focusing on PDP as both cortical and white matter structures is a novel perspective, but more extensive studies are necessary to fully elucidate their connectivity patterns and functional roles.

Additionally, our process of marking the PDP observed in the cadaver brains onto the template surface may have limitations. Specifically, we directly marked them on the template brain (see Fig. 2A). While similar processes have been used before, such as mapping histological parcellations onto the standard MNI brain¹ and lesion locations from case reports to standard MNI brain space,^{5–7} it is indeed true that inter-individual variability of gyral and sulcal anatomy cannot be accounted for by this method. Our approach is more probabilistic (as described in Fig. 2A), mapping average locations of the PDP (as found in cadavers) onto the average brain space (as defined by the MNI template), similar to using an average group connectome based on resting-state fMRI scans from normal brains.¹²

Regarding the imaging resolution, the fMRI scans used to create the normative functional connectome had a voxel size of between 2.0 and 2.4 mm isotropic, with no gap between slices. It is key to emphasize that the seeds were run along 812 to >4000 scans and the results were averaged. These datasets are widely used, and are the same group-average resting-state datasets in which SCAN was previously described by Gordon et al.²¹

Our study included MEP recordings following stimulations of the PDP-related sites on the central sulcus. While this data is valuable, we were not able to assess these connections in awake patients; as such, we might have missed critical insights that could only be captured through conscious responses during specific tasks.

While our findings suggest that PDP may have implications for enhancing therapeutic outcomes in neuromodulation and surgical interventions, particularly in conditions such as neuropathic pain, Parkinson's disease and complex motor cortex-situated tumours, clinical trials and additional research are needed to confirm these potential applications. Future studies should aim to increase sample sizes, utilize longitudinal data to track changes over time, and to explore the mechanistic underpinnings of PDP involvement in broader neural networks.

Another limitation of this study is the lack of information on post-mortem times and the cause of death of the donors whose hemispheres were used in the fibre microdissections. Nevertheless, when we receive cadavers in our lab, we ensure that the brains do not come from donors with neuropsychiatric disorders by excluding those with known neurological diseases or causes of death related to neurological conditions. This exclusion is based on the information provided in the official documentation we receive, which includes a log of known diseases and the cause of death as well as gross inspection of the brains. Additionally, we conduct a thorough morphological examination to confirm that there are no abnormalities or lesions indicative of gross disease or previous stroke. Cadavers that do not meet these criteria are excluded from our studies.

Data availability

Functional MRI data used in this study are available online (<http://neuroinformatics.harvard.edu/gsp/>). Patient data are available as [Supplementary material](#). Imaging data used in this study are publicly available through the human connectome project (<https://www.humanconnectome.org/>) and DSI studio (<https://dsi-studio.labsolver.org/>). Human cadaver data are not publicly available for privacy reasons.

Funding

The tractographic tool used in this study is partly supported by National Institutes of Health grant R01 NS120954. This work was

supported by National Institutes of Health grants MH096773 (NUFD), MH122066 (EMG, NUFD), MH121276 (EMG, NUFD), MH124567 (EMG, NUFD), NS129521 (EMG, NUFD), and NS088590 (NUFD); by the Intellectual and Developmental Disabilities Research Center (NUFD); by the Kiwanis Foundation (NUFD); and by the Washington University Hope Center for Neurological Disorders (EMG, NUFD). A.H. was supported by the German Research Foundation (Deutsche Forschungsgemeinschaft, 424778381—TRR 295), Deutsches Zentrum für Luft- und Raumfahrt (DynaSti grant within the EU Joint Programme Neurodegenerative Disease Research, JPND), the National Institutes of Health (R01 13478451, 1R01NS127892-01, 2R01 MH113929 and UM1NS132358) as well as the New Venture Fund (FFOR Seed Grant).

Competing interests

N.U.F.D. has a financial interest in Turing Medical Inc. and may financially benefit if the company is successful in marketing FIRMM motion monitoring software products. E.M.G. and N.U.F.D. may receive royalty income based on FIRMM technology developed at Washington University School of Medicine and licensed to Turing Medical Inc. N.U.F.D. is a co-founder of Turing Medical Inc. These potential conflicts of interest have been reviewed and are managed by Washington University School of Medicine. A.H. reports lecture fees for Boston Scientific and is a consultant for FxNeuromodulation and Abbott.

Supplementary material

[Supplementary material](#) is available at *Brain* online.

References

1. Rathelot JA, Strick PL. Subdivisions of primary motor cortex based on cortico-motoneuronal cells. *Proc Natl Acad Sci U S A*. 2009;106:918–923.
2. Piotrowska N, Winkler PA. Otfried Foerster, the great neurologist and neurosurgeon from Breslau (Wrocław): His influence on early neurosurgeons and legacy to present-day neurosurgery. *J Neurosurg*. 2007;107:451–456.
3. Penfield W, Boldrey E. Somatic motor and sensory representation in the cerebral cortex of man as studied by electrical stimulation. *Brain*. 1937;60:389–443.
4. Gray GW. The great ravelled knot. *Sci Am*. 1948;179:26–39.
5. Kandel ER, Koester JD, Mack SH, Siegelbaum SA. *Principles of neural science*. 6th edition. McGraw Hill; 2021.
6. Blumenfeld H. *Neuroanatomy through clinical cases*. Oxford University Press; 2021.
7. Hamani C, Fonoff ET, Parravano DC, et al. Motor cortex stimulation for chronic neuropathic pain: Results of a double-blind randomized study. *Brain*. 2021;144:2994–3004.
8. Dimyan MA, Cohen LG. Neuroplasticity in the context of motor rehabilitation after stroke. *Nat Rev Neurol*. 2011;7:76–85.
9. Joy MT, Carmichael ST. Activity-dependent transcriptional programs in memory regulate motor recovery after stroke. *Commun Biol*. 2024;7:1–16.
10. Viganò L, Howells H, Rossi M, et al. Stimulation of frontal pathways disrupts hand muscle control during object manipulation. *Brain*. 2022;145:1535–1550.
11. Rossi M, Viganò L, Puglisi G, et al. Targeting primary motor cortex (M1) functional components in M1 gliomas enhances safe

- resection and reveals M1 plasticity potentials. *Cancers (Basel)*. 2021;13:3808.
12. Mantovani A, Rossi S, Bassi BD, Simpson HB, Fallon BA, Lisanby SH. Modulation of motor cortex excitability in obsessive-compulsive disorder: An exploratory study on the relations of neurophysiology measures with clinical outcome. *Psychiatry Res*. 2013;210:1026–1032.
 13. Hamer HM, Reis J, Mueller HH, et al. Motor cortex excitability in focal epilepsies not including the primary motor area—A TMS study. *Brain*. 2005;128(Pt 4):811–818.
 14. White LE, Andrews TJ, Hulette C, et al. Structure of the human sensorimotor system. I: Morphology and cytoarchitecture of the central sulcus. *Cereb Cortex*. 1997;7:18–30.
 15. Geyer S, Ledberg A, Schleicher A, et al. Two different areas within the primary motor cortex of man. *Nature*. 1996;382:805–807.
 16. Van Essen DC, Glasser MF, Dierker DL, Harwell J, Coalson T. Parcellations and hemispheric asymmetries of human cerebral cortex analyzed on surface-based atlases. *Cereb Cortex*. 2012;22:2241–2262.
 17. Gratiolet P. *Mémoire sur les plis cérébraux de l'homme et des primates: Mit einem atlas*. Volume 1. A. Bertrand; 1854: pp. XIV pl. in fol. 33i.
 18. Broca P. *Mémoires d'anthropologie zoologique et biologique*. Volume 3. C. Reinwald et Cie.; 1877.
 19. Olivier A, Boling WW, Tanriverdi T. *Techniques in epilepsy surgery: The MNI approach*. Cambridge University Press; 2012.
 20. Bodin C, Pron A, Le Mao M, Régis J, Belin P, Coulon O. Plis de passage in the superior temporal sulcus: Morphology and local connectivity. *Neuroimage*. 2021;225:117513.
 21. Gordon EM, Chauvin RJ, Van AN, et al. A somato-cognitive action network alternates with effector regions in motor cortex. *Nature*. 2023;617:351–359.
 22. Jensen MA, Huang H, Valencia GO, et al. A motor association area in the depths of the central sulcus. *Nat Neurosci*. 2023;26:1165–1169.
 23. Dosenbach NUF, Raichle ME, Gordon E. The brain's cingulo-opercular action-mode network. [Preprint] *PsyArXiv*. <https://osf.io/preprints/psyarxiv/2vt79>
 24. Miller KL, Alfaro-Almagro F, Bangerter NK, et al. Multimodal population brain imaging in the UK Biobank prospective epidemiological study. *Nat Neurosci*. 2016;19:1523–1536.
 25. Casey BJ, Cannonier T, Conley MI, et al. The adolescent brain cognitive development (ABCD) study: Imaging acquisition across 21 sites. *Dev Cogn Neurosci*. 2018;32:43–54.
 26. Glasser MF, Smith SM, Marcus DS, et al. The human connectome project's neuroimaging approach. *Nat Neurosci*. 2016;19:1175–1187.
 27. Petersen S, Schlaggar B, Power J. Washington University 120. OpenNeuro; 2018. <https://openneuro.org/datasets/ds000243/>
 28. Graziano MSA. Ethological action maps: A paradigm shift for the motor cortex. *Trends Cogn Sci*. 2016;20:121–132.
 29. Dum RP, Levinthal DJ, Strick PL. Motor, cognitive, and affective areas of the cerebral cortex influence the adrenal medulla. *Proc Natl Acad Sci U S A*. 2016;113:9922–9927.
 30. Skandalakis GP, Komaitis S, Kalyvas A, et al. Dissecting the default mode network: Direct structural evidence on the morphology and axonal connectivity of the fifth component of the cingulum bundle. *J Neurosurg*. 2020;134:1334–1345.
 31. Skandalakis GP, Neudorfer C, Payne CA, et al. Establishing connectivity through microdissections of midbrain stimulation-related neural circuits. *Brain*. 2024;147:3083–3098.
 32. Skandalakis GP, Linn WJ, Yeh FC, et al. Unveiling the axonal connectivity between the precuneus and temporal pole: Structural evidence from the cingulum pathways. *Hum Brain Mapp*. 2024;45:e26771.
 33. Eickhoff SB, Heim S, Zilles K, Amunts K. Testing anatomically specified hypotheses in functional imaging using cytoarchitectonic maps. *Neuroimage*. 2006;32:570–582.
 34. Glasser MF, Sotiropoulos SN, Wilson JA, et al. The minimal pre-processing pipelines for the human connectome project. *Neuroimage*. 2013;80:105–124.
 35. Marek S, Tervo-Clemmens B, Calabro FJ, et al. Reproducible brain-wide association studies require thousands of individuals. *Nature*. 2022;603:654–660.
 36. Robinson EC, Jbabdi S, Glasser MF, et al. MSM: A new flexible framework for multimodal surface matching. *Neuroimage*. 2014;100:414–426.
 37. Smith SM, Beckmann CF, Andersson J, et al. Resting-state fMRI in the human connectome project. *Neuroimage*. 2013;80:144–168.
 38. Rossi M, Sciortino T, Conti Nibali M, et al. Clinical pearls and methods for intraoperative motor mapping. *Neurosurgery*. 2021;88:457–467.
 39. Fornia L, Ferpozzi V, Montagna M, et al. Functional characterization of the left ventrolateral premotor cortex in humans: A direct electrophysiological approach. *Cereb Cortex*. 2018;28:167–183.
 40. Fischl B. FreeSurfer. *Neuroimage*. 2012;62:774–781.
 41. Tadel F, Baillet S, Mosher JC, Pantazis D, Leahy RM. Brainstorm: A user-friendly application for MEG/EEG analysis. *Comput Intell Neurosci*. 2011;2011:879716.
 42. Eickhoff SB, Stephan KE, Mohlberg H, et al. A new SPM toolbox for combining probabilistic cytoarchitectonic maps and functional imaging data. *Neuroimage*. 2005;25:1325–1335.
 43. Eickhoff SB, Paus T, Caspers S, et al. Assignment of functional activations to probabilistic cytoarchitectonic areas revisited. *Neuroimage*. 2007;36:511–521.
 44. Bellacicca A, Rossi M, Viganò L, et al. Peaglet: A user-friendly probabilistic kernel density estimation of intracranial cortical and subcortical stimulation sites. *J Neurosci Methods*. 2024;408:110177.
 45. Yeh FC. Population-based tract-to-region connectome of the human brain and its hierarchical topology. *Nat Commun*. 2022;13:4933.
 46. Ben Shalom D, Skandalakis GP. Four streams within the prefrontal cortex: Integrating structural and functional connectivity. *Neuroscientist*. Published online 5 April 2024. doi:10.1177/10738584241245304
 47. Skandalakis GP, Barrios-Martinez J, Kazim SF, et al. The anatomy of the four streams of the prefrontal cortex. Preliminary evidence from a population based high definition tractography study. *Front Neuroanat*. 2023;17:1214629.
 48. Bajada CJ, Schreiber J, Caspers S. Fiber length profiling: A novel approach to structural brain organization. *Neuroimage*. 2019;186:164–173.
 49. Krubitzer L, Huffman KJ, Disbrow E, Recanzone G. Organization of area 3a in macaque monkeys: Contributions to the cortical phenotype. *J Comp Neurol*. 2004;471:97–111.
 50. Honey CJ, Sporns O, Cammoun L, et al. Predicting human resting-state functional connectivity from structural connectivity. *Proc Natl Acad Sci U S A*. 2009;106:2035–2040.
 51. Park HJ, Friston K. Structural and functional brain networks: From connections to cognition. *Science*. 2013;342:1238411.
 52. Damoiseaux JS, Greicius MD. Greater than the sum of its parts: A review of studies combining structural connectivity and resting-state functional connectivity. *Brain Struct Funct*. 2009;213:525–533.

53. Kalyvas A, Koutsarnakis C, Komaitis S, et al. Mapping the human middle longitudinal fasciculus through a focused anatomic-imaging study: Shifting the paradigm of its segmentation and connectivity pattern. *Brain Struct Funct*. 2020;225:85-119.
54. Komaitis S, Skandalakis GP, Kalyvas AV, et al. Dorsal component of the superior longitudinal fasciculus revisited: Novel insights from a focused fiber dissection study. *J Neurosurg*. 2019;132:1265-1278.
55. Catani M, Jones DK, ffytche DH. Perisylvian language networks of the human brain. *Ann Neurol*. 2005;57:8-16.
56. Desmurget M, Song Z, Mottolese C, Sirigu A. Re-establishing the merits of electrical brain stimulation. *Trends Cogn Sci*. 2013;17:442-449.
57. Penfield W. The cerebral cortex in man: I. The cerebral cortex and consciousness. *Arch Neurol Psychiatry*. 1938;40:417-442.
58. Penfield W, Welch K. The supplementary motor area of the cerebral cortex; a clinical and experimental study. *AMA Arch Neurol Psychiatry*. 1951;66:289-317.
59. Penfield W, Welch K. Instability of response to stimulation of the sensorimotor cortex of man. *J Physiol*. 1949;109:358-365.
60. Overduin SA, d'Avella A, Carmena JM, Bizzi E. Microstimulation activates a handful of muscle synergies. *Neuron*. 2012;76:1071-1077.
61. Ren J, Zhang W, Dahmani L, et al. The somato-cognitive action network links diverse neuromodulatory targets for Parkinson's disease. [Preprint] *BioRxiv*. <https://doi.org/10.1101/2023.12.12.571023>